

# Polarization Analysis of an Asymmetrically Etched Rib Waveguide Coupler for Sensing Applications

Malathi SATHISH\* and Srinivas TALABATTULA

*Applied Photonics Lab, Department of Electrical & Communication Engineering, Indian Institute of Science, Bangalore, 560012, India*

\*Corresponding author: Malathi SATHISH      E-mail: sathishvac@gmail.com

**Abstract:** Deeply etched rib waveguides on silicon on insulator platform were not addressed well in research publications. We have analyzed single mode condition and polarization independence of a deeply etched rib waveguide (DE-RW) structure from biosensing perspective. With this rib structure, an asymmetrically etched integrated optic directional coupler has been numerically modeled to have the same coupling length for quasi- TE and TM modes. The coupling coefficients with the glucose solution as an upper cladding were calculated using a full vector mode solver, and the bulk refractive index sensitivity of the sensor was found as  $28.305 \times 10^{-2}$ /RIU for a fundamental quasi-TE mode.

**Keywords:** Silicon on insulator (SOI), deeply etched rib waveguide, asymmetrically etched, directional coupler, biosensor

Citation: Malathi SATHISH and Srinivas TALABATTULA, "Polarization Analysis of an Asymmetrically Etched Rib Waveguide Coupler for Sensing Applications," *Photonic Sensors*, vol. 3, no. 2, pp. 178–183, 2013.

## 1. Introduction

Directional couplers (DCs) are formed by placing two integrated optic waveguides in close proximity. Initially, researchers worked on couplers fabricated with lithium niobate, GaAs, InP or SiO<sub>2</sub> [1] waveguides which normally had a larger cross section. Those structures demanded a wide gap between waveguides and hence pushed the coupling length limit to the millimeter and centimeter range. High index contrast of silicon on insulator (SOI) platform facilitated us to fabricate miniaturized devices that were compatible with the well developed and documented complementary metal-oxide-semiconductor (CMOS) technology. Silicon rib and strip (Si wire) geometry offers an advantage of confining light in a very small

dimension. Hence, silicon rib/strip waveguides are widely used in telecommunications and sensing applications. Strip waveguides find application in devices requiring long propagation lengths and bends, while waveguides with a larger cross section such as rib waveguides are used in short straight integrated optic devices [2]. Rib waveguides with 1- $\mu\text{m}$  height support single mode propagation, where as strip waveguides with 250-nm height would become multimodal. The larger cross section of rib structures enables us to achieve low fiber coupling losses compared to strip structures.

Directional couplers are essential to design ring resonators or racetrack resonators that support phase matched TE and TM modes for bio sensing applications. The motive of this research work was to compute the coupler length which yielded the

same level of power transfer for both polarizations. Hence, we focused on polarization independent rib waveguide couplers in this work. We were addressing the least explored device; deeply etched rib waveguide (DE-RW) based directional couplers with asymmetrical etching from a bio sensing perspective in this paper. Soref *et al.* [3] proposed an expression for the single mode condition (SMC) for rib waveguides based on their geometry given by (1a) and (1b):

$$\frac{W}{H} \leq \alpha + \frac{r}{\sqrt{1-r^2}} \quad (1a)$$

$$r = \frac{h}{H} \geq 0.5 \quad (1b)$$

where  $W$  and  $H$  are the width and height of the rib waveguide. The symbol  $h$  represents the slab height, and the value of  $\alpha$  is 0.3. The second criterion restricts the rib structure to be shallowly etched ( $r \geq 0.5$ ). Soref and his team predicted that higher order modes in the rib region would possess effective indices lesser than the fundamental mode of the slab section. Hence, higher order modes of the rib region get coupled to slab modes and suffer higher propagation losses.

Later, Pogossian *et al.* [4] compared experimental results with the effective index method (EIM) and proposed a similar equation. They claimed that the value of  $\alpha$  in (1a) was zero instead of 0.3 as a condition for single mode propagation. Lousteau *et al.* [5] in their work highlighted the necessity for numerical analysis along with Soref's equations. Most of the literature published so far focused mainly on shallowly etched rib waveguides except a few papers [6, 7]. Researchers have demonstrated numerically and experimentally the asymmetrical configuration of rib waveguide directional couplers on a large device layer [8]. We have analyzed the directional coupler formed with the least explored deeply and asymmetrically etched rib waveguide configuration and their application as a bio sensor.

This work apprehended the significance of three

domains, viz., (1) single mode condition of DE-RW with the bio clad, (2) the asymmetrically etched rib waveguide coupler, and (3) condition for polarization independence. Section 2 deals with single mode condition of the DE-RW, Section 3 delineates polarization independence of an asymmetrically etched directional coupler, Section 4 describes about glucose sensing, and the last section covers conclusions drawn from various analyses.

## 2. Waveguide design

For evanescent sensing applications, the waveguide should be mono-modal. If multi-modes are allowed to propagate, each mode would interact with the upper clad (bio material) and create interference during information retrieval. In previous section, we have highlighted the fact that Soref's conditions (1a) and (1b) were limited only to shallowly etched structures. Hence, we began with an analysis for the single mode condition of a DE-RW by the semi analytical method and full vectorial method using the eigen mode solver<sup>TM</sup> tool from Lumerical [9].

We adopted the EIM for the whole structure after solving three slab regions using the transfer matrix method (TMM) based MATLAB codes developed by H. P. Uranus [10]. The eigen mode solver meshes a given geometry and solves Maxwell's equations by the finite difference algorithm. The schematic diagram of a DE-RW structure is shown in Fig. 1.

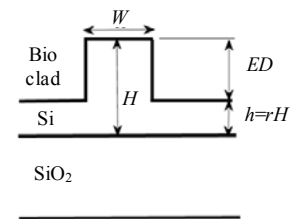


Fig. 1 Schematic diagram of a deeply etched rib waveguide.

Here,  $W$ ,  $H$ ,  $h$  and  $ED$  represent the width, rib height, slab height and etch depth, respectively. In the simulation, we kept the refractive index of silicon (core) as 3.477, silica (buffer/lower cladding) as 1.444 and upper cladding (biomaterial) as 1.33. For

a range of etch depths ( $0.25\ \mu\text{m}$ – $0.5\ \mu\text{m}$ ), we varied the rib width in steps of  $0.01\ \text{nm}$  till the second mode appeared to find the maximum width that satisfied mono-modal condition. The comparison of the semi analytical method and eigen mode solver method is plotted in Fig. 2.

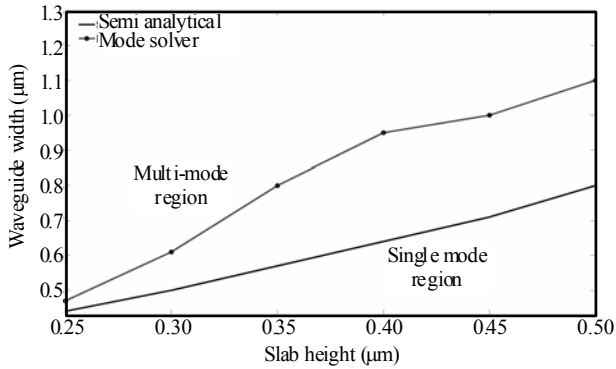
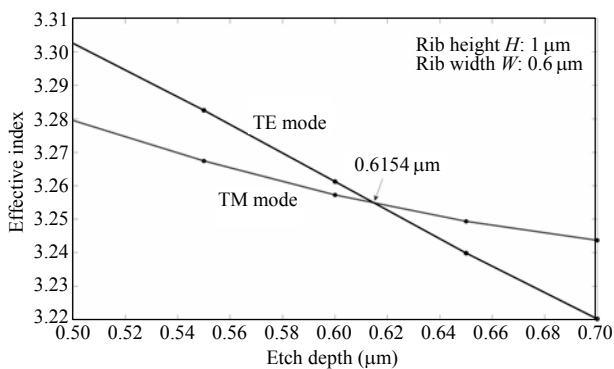
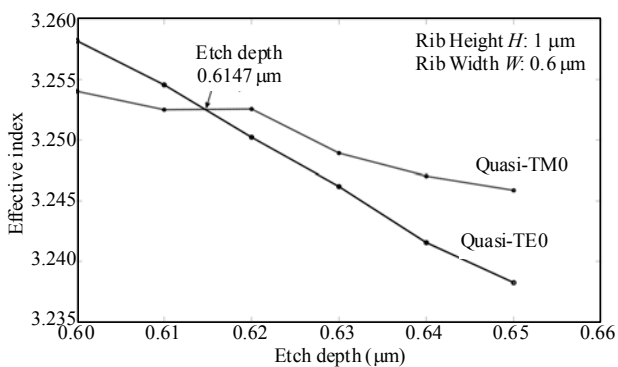


Fig. 2 Single mode condition of a DE-RW with the bio clad.



(a)



(b)

Fig. 3 Polarization independence analysis by the (a) non-uniform mesh finite difference (FD) method [11] and (b) eigen mode solver method.

Before designing the polarization insensitive directional coupler, we needed to ascertain the

birefringence of the DE-RW. We adopted the full vector finite difference scheme with the non-uniform mesh rib analysis [11] that calculated effective indices of fundamental quasi-TE and quasi-TM modes. We varied the etch depth of the DE-RW while ensuring SMC by fixing the waveguide width to be  $0.6\ \mu\text{m}$  and analyzed the birefringence condition. From Fig. 3(a), it could be inferred that at an etch depth of  $0.6154\ \mu\text{m}$ , both TE and TM modes of the DE-RW had same effective indices. The eigen mode simulation results varied marginally from finite difference analysis as depicted in Fig. 3(b), and the birefringence etch depth turned out to be  $0.6147\ \mu\text{m}$ . Considering fabrication issues, authors have fixed the etch depth of the DE-RW as  $0.62\ \mu\text{m}$  (slab height  $h$ :  $0.38\ \mu\text{m}$ ) throughout subsequent simulations of their work.

### 3. Directional coupler design and simulation

Here, we compare symmetrically and asymmetrically etched directional couplers formed using DE-RW structures with the bio material clad. Conventions used in Fig. 4 are same as DE-RW geometry, and  $G$  represents the gap between waveguides. In the simulation of bulk refractive index sensing, we assumed a uniform upper cladding. The quasi-TE mode had higher amplitude at side walls; hence we focused on TE mode coupling characteristics which were more sensitive to the gap between two adjacent waveguides.

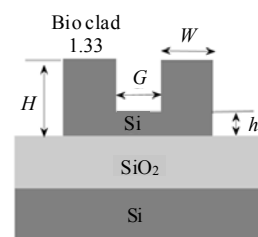


Fig. 4 Cross-sectional view of an asymmetrically etched directional coupler.

Designing a polarization independent coupler makes the coupling length equal for both polarizations. Figures 5(a) and 5(b) show a typical result of modeling conventional and asymmetrically

etched directional couplers using the eigen mode solver, respectively. The silicon on insulator directional coupler exhibits birefringence at the 110-nm gap, whereas asymmetrically etched rib coupler’s fundamental TE and TM mode coupling length curves do not intersect as shown in Fig.5(b). We found that the coupling length related to the quasi-TE mode was shorter than that to the TM, hence plotted three fold power exchange curves of a TE mode. Now we could figure out birefringence points on both curves by adopting a method suggested in literature [12]. Three sets of gaps (coupling strength), viz., 100nm, 500nm and 900nm were selected, and both types of the DC were studied.

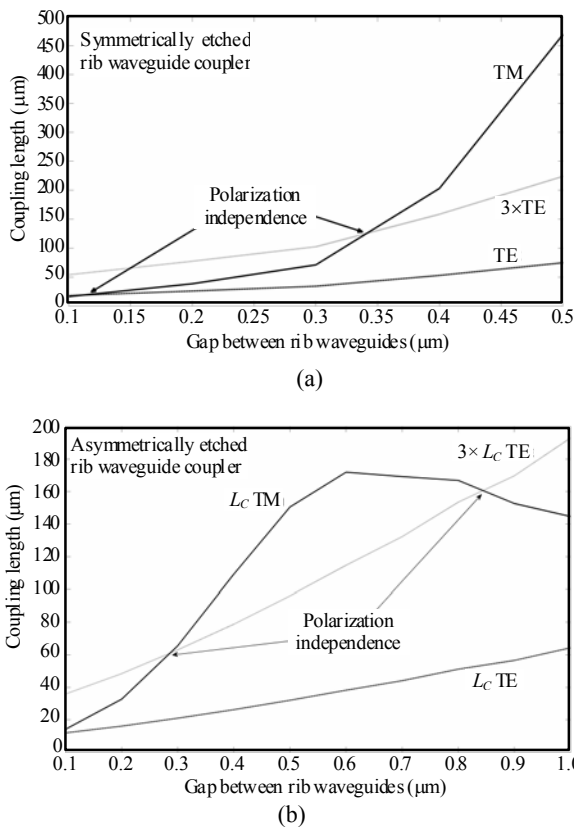


Fig.5 Polarization study of directional couplers: (a) symmetrically etched and (b) asymmetrically etched configurations.

We have tabulated investigations made by varying the gap between waveguides to achieve the polarization independent DC in Table.1. We found a significant improvement in the coupling distance when we etched the coupler asymmetrically. The discrepancy increased as the gap between

waveguides increased from a few hundred nanometers to micrometer. From last two rows of the table, it could be inferred that by asymmetrical etching, the coupling length reduced substantially to half of the symmetrical DC’s length.

Table 1 Comparison of symmetrically etched and asymmetrically etched directional couplers.

Etching type	Gap (nm)	Cross coupling length (μm)
Symmetrical DC	340	126
Asymmetrical DC	283	62

We compared the proposed deeply and asymmetrically etched rib waveguide coupler with published results [8]. The coupling length reported by Cao *et al.* was 360μm for a gap of 1μm where as in our case we achieved 154μm. In this method, we reduced the cross section of the waveguide by (1) reducing the thickness of the silicon device layer to 1μm and (2) deeply etching the rib waveguide while maintaining single mode and polarization independence.

#### 4. Glucose sensing

Fiber based sensors and fiber Bragg grating devices are promising solutions in the sensing domain [13–15]. In our simulations, we considered the proposed integrated optic directional coupler as a biosensor. We simulated a bulk sensing environment with the glucose solution as the upper clad on the optimized device (deeply and asymmetrically etched DC). The schematic diagram of the coupler is represented in Fig.6, where *Pin* and *G* denote the input power and gap between waveguides, respectively. In our simulations, the fundamental quasi-TE mode was launched at a wavelength of 1550nm. We varied refractive indices of the solution from 1.333 to 1.3344 with different glucose concentrations [16].

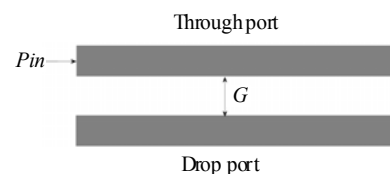


Fig.6 Schematic of a directional coupler.

We calculated the coupling coefficient  $\kappa$  in accordance with the coupled mode theory (CMT) as indicated in (2):

$$\kappa = \frac{1}{2}(\beta_s - \beta_a) \quad (2)$$

where  $\beta_s$  and  $\beta_a$  are propagation constants of symmetric and anti-symmetric modes the directional coupler, respectively. Using the eigen mode solver, we performed the modal analysis to calculate above mentioned propagation constants with various glucose concentrations as the upper cladding. From a set of  $\kappa$ , we estimated the coupling distance  $L_C$  using the following expression:

$$L_C = \frac{\pi}{2\kappa}. \quad (3)$$

The normalized power flowing in the through port is given by (4), and by replacing the cosine function of this expression with a sine function, we get the drop port power:

$$\frac{P_{\text{thro}}}{P_{\text{in}}} = \cos^2\left(\frac{\pi L}{2 L_C}\right). \quad (4)$$

The through port power response of the proposed DC, the corresponding curve fitting model and equation are shown in Fig. 7. The proposed device had a sensitivity of  $28.305 \times 10^{-2}$ /RIU for the quasi-TE mode.

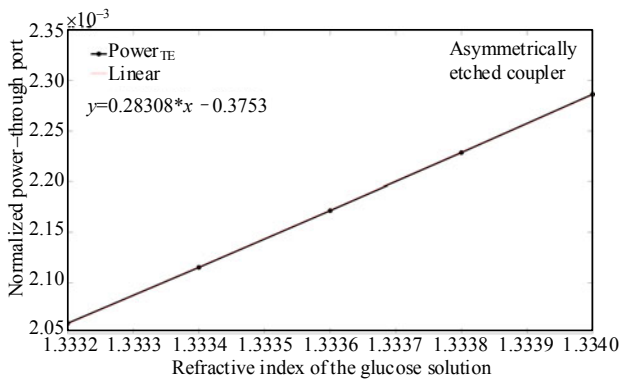


Fig. 7 Normalized power response of the optimized DC with the glucose solution.

## 5. Conclusions

We proposed and analyzed an asymmetrically etched directional coupler with the DE-RW. Initially,

we examined the single mode condition of the DE-RW with the bio environment and then optimized rib geometry to achieve polarization independence. Finally, we looked into the performance of the optimized device for glucose sensing applications. The optimized device had a sensitivity of  $28.305 \times 10^{-2}$ /RIU for a fundamental quasi-TE mode. Due to polarization independent geometry, one could expect the same performance for quasi-TM mode propagation. Our future work involves the study of the racetrack resonator formed with this structure in the coupling area and the analysis of its spectral response.

## Acknowledgment

One of the authors, Malathi SATHISH, would like to thank Dr. Murugesan Venkatapathi and all research students of Applied Photonics and Computational Photonics Labs, Indian Institute of Science, Bangalore, for their technical support in simulation work.

**Open Access:** This article is distributed under the terms of the Creative Commons Attribution License which permits any use, distribution, and reproduction in any medium, provided the original author(s) and source are credited.

## References

- [1] B. J. Luff, R. D. Harris, J. S. Wilkinson, R. Wilson, and D. J. Schiffrin, "Integrated optical directional coupler biosensor," *Optics Letters*, vol. 21, no. 8, pp. 618–620, 1996.
- [2] M. Lipson, "Guiding, modulating, and emitting light on silicon – challenges and opportunities," *Journal of Lightwave Technology*, vol. 23, no. 12, pp. 4222–4237, 2005.
- [3] R. A. Soref, J. Schmidtchen, and K. Petermann, "Large single-mode rib waveguides in Ge-Si and Si-on-SiO<sub>2</sub>," *IEEE Journal of Quantum Electronics*, vol. 27, no. 8, pp. 1971–1974, 1991.
- [4] S. P. Pogossian, L. Vescan, and A. Vonsovici, "The single mode condition for semiconductor rib waveguides with large large cross section," *Journal of*

- Lightwave Technology*, vol. 16, no. 10, pp. 1851–1853, 1998.
- [5] J. Lousteau, D. Furniss, A. B. Seddon, T. M. Benson, A. Vukovic, and P. Sewell, “The single-mode condition for silicon-on-insulator optical rib waveguides with large cross section,” *Journal of Lightwave Technology*, vol. 22, no. 8, pp. 1923–1929, 2004.
- [6] L. Vivien, S. Laval, B. Dumont, S. Lardenois, A. Koster, and E. Cassan, “Polarization-independent single-mode rib waveguides on silicon-on-insulator for telecommunication wavelengths,” *Optics Communications*, vol. 210, no. 1–2, pp. 43–49, 2002.
- [7] S. P. Chan, C. E. Png, S. T. Lim, G. T. Reed, and V. M. N. Passaro, “Single-mode and polarization – independent silicon-on-insulator waveguides with small cross section,” *Journal of Lightwave Technology*, vol. 23, no. 6, pp. 2103–2111, 2005.
- [8] G. B. Cao, F. Gao, J. Jiang, and F. Zhang, “Directional couplers realized on silicon-on-insulator,” *IEEE Photonics Technology Letters*, vol. 17, no. 8, pp. 1671–1673, 2005.
- [9] J. Klein and J. Pond, “Simulation and optimization of photonic integrated circuits,” in *20th Integrated Photonics Research, Silicon and Nanophotonics conference*, United States, June 17–22, pp. IM2B.2, 2012.
- [10] H. P. Uranus, H. Hoekstra, and E. Van Groesen, “Finite difference scheme for planar waveguides with arbitrary index profiles and its implementation for anisotropic waveguides with a diagonal permittivity tensor,” *Optical and Quantum Electronics*, vol. 35, no. 4, pp. 407–427, 2003.
- [11] A. B. Fallahkhair, K. S. Li, and T. E. Murphy, “Vector finite difference mode solver for anisotropic dielectric waveguides,” *Journal of Lightwave Technology*, vol. 26, no. 11, pp. 1423–1431, 2008.
- [12] W. R. Headley, G. T. Reed, S. Howe, A. Liu, and M. Paniccia, “Polarization-independent optical racetrack resonators using rib waveguides on silicon-on-insulator,” *Applied Physics Letters*, vol. 85, no. 23, pp. 5523–5525, 2004.
- [13] K. S. Chiang, Y. Q. Liu, Q. Liu, and Y. J. Rao, “Optical sensing based on light coupling between two parallel long-period fiber gratings,” *Photonic Sensors*, vol. 1, no. 3, pp. 204–209, 2011.
- [14] A. P. Zhang, S. R. Gao, G. F. Yan, and Y. B. Bai, “Advances in optical fiber Bragg grating sensor technologies,” *Photonic Sensors*, vol. 2, no. 1, pp. 1–13, 2012.
- [15] M. H. Yang and J. X. Dai, “Review on optical fiber sensors with sensitive thin films,” *Photonic Sensors*, vol. 2, no. 1, pp. 14–28, 2012.
- [16] L. M. Lechuga, “Integrated optical silicon IC compatible nano devices for bio sensing application,” in *Proc. SPIE*, vol. 5119, pp. 140–148, 2003.